The JHU Turbulence Databases (*JHTDB*)

STABLY-STRATIFIED ATMOSPHERIC BOUNDARY-LAYER TURBULENCE ON A 2048^3 GRID

Data provenance: P. P. Sullivan[1] and E. G. Patton[1]

Database ingest and Web services: A. Lubonja [2], M. Schnaubelt [2], H. Yao[2], G. Lemson[2], R. Burns[2], A. Szalay[2], C. Meneveau[2], and IDIES staff

[1]NSF National Center for Atmospheric Research, Boulder, CO 80301

[2]Johns Hopkins University, Baltimore, MD 21218

The data is from an atmospheric large-eddy simulation (LES) of the GABLS1 intercomparison case originally described by Holtslag (2006) and Beare et al. (2006). The problem design provides an excellent test-bed to study stratified turbulence in a high-Reynolds-number boundary-layer flow using large-eddy simulation (LES).

The first GABLS1 intercomparison used LES models with coarse and fine meshes of $N = 128^3$ and 200^3 gridpoints (Beare et al., 2006; Huang and Bou-Zeid, 2013), suitable for the computational capabilities at that time; flow was forced by specifying a geostrophic windspeed $U_g = 8$ m s^{-1} and a surface cooling rate $C_r = 0.25$ K h^{-1}. Although there was qualitative agreement amongst the LES models, there are hints that an increased resolution resulted in shallower SBLs inducing a change in the surface friction velocity u_* and surface cooling flux Q_*. This motivated further study and Sullivan et al. (2016) explored the LES solution sensitivity using meshes of $N = (200^3, 512^3, 1024^3)$ gridpoints along with four different cooling rates $C_r = (0.25, 0.375, 0.5, 1.0)$ K h^{-1}. Here we advance the work presented in Sullivan et al. (2016) by providing data from LES of the GABLS1 configuration for a cooling rate of $C_r = 0.25$ K h^{-1} using $N = 2048^3$ gridpoints (McWilliams et al., 2023).

Governing equations: The model equations for large-eddy simulation of a stably-stratified atmospheric boundary layer (SBL) under the Boussinesq approximation with system rotation and with a flat bottom boundary are:

$$\frac{\partial \overline{\mathbf{u}}}{\partial t} + \overline{\mathbf{u}}\cdot\nabla\overline{\mathbf{u}} = -\mathbf{f}\times(\overline{\mathbf{u}}-\mathbf{U}_g) - \nabla\overline{\pi} + \hat{\mathbf{z}}\beta(\overline{\theta}-\theta_{\mathrm{ref}}) - \nabla\cdot\mathbf{T} \tag{1a}$$

$$\frac{\partial \overline{\theta}}{\partial t} + \overline{\mathbf{u}}\cdot\nabla\overline{\theta} = -\nabla\cdot\mathbf{B} \tag{1b}$$

$$\frac{\partial e}{\partial t} + \overline{\mathbf{u}}\cdot\nabla e = \mathcal{P} + \mathcal{B} + \mathcal{D} - \mathcal{E} \tag{1c}$$

$$\nabla\cdot\overline{\mathbf{u}} = 0\,. \tag{1d}$$

The equation set includes transport equations for: momentum $\rho\overline{\mathbf{u}}$ (1a); potential temperature $\overline{\theta}$ (1b); and subfilter-scale (SFS) turbulent kinetic energy e (1c). The divergence-free (incompressible) condition (1d) determines the elliptic pressure variable $\overline{\pi}$. The variables that appear in (1) are: velocity components

$\overline{\mathbf{u}} \equiv \overline{u}_i = (\overline{u}, \overline{v}, \overline{w})$, geostrophic winds $\mathbf{U}_g = (U_g, V_g)$, rotation vector $\mathbf{f} = (0, 0, f)$ with Coriolis parameter f, unit vector $\hat{\mathbf{z}}$ in the vertical direction, and buoyancy parameter $\beta = g/\theta_{\text{ref}}$, where g is gravity and θ_{ref} is a reference temperature. Pressure $\overline{p}$ and air density ρ do not appear explicitly in (1). The terms on the right-hand side of (1c) for e are shear production $\mathcal{P}$, buoyancy production–destruction $\mathcal{B}$, diffusion $\mathcal{D}$, and dissipation $\mathcal{E}$. The modeling of these terms is described in Moeng and Sullivan (2015). The overbar notation $\overline{(\,)}$ denotes a spatially filtered quantity.

The LES equations are formally derived by applying a spatial filter term-by-term to the governing equations of motion. This operation introduces the unknown SFS kinematic momentum and temperature fluxes

$$\mathbf{T} \equiv \tau_{ij} = \overline{u_i u_j} - \overline{u}_i \overline{u}_j \quad ; \quad \mathbf{B} \equiv B_i = \overline{u_i \theta} - \overline{u}_i \overline{\theta} \tag{2}$$

For the SBL we adopt the two-part SFS model proposed by Sullivan et al. (1994), which utilizes the transport equation (1c) and an eddy viscosity approach to parameterize the SFS fluxes given by (2). This parameterization is specifically tailored to a high-Reynolds-number LES that uses rough-wall surface boundary conditions based on Monin–Obukhov (MO) similarity theory. For momentum, the subgrid eddy viscosity prescription $\nu_{t_M} = C_e \gamma \sqrt{e}\, \ell$, where the coefficient is set to its standard value $C_e = 0.1$ and ℓ is a length scale characteristic of the subgrid turbulence. For temperature, $\nu_{t_\theta} = [1 + (2\ell/\Delta)]\nu_{t_M}$. Typically $\ell = \Delta$, where Δ is the filter width defined by the LES grid and the explicit dealiasing associated with the pseudospectral differencing of the NCAR-LES such that

$$\Delta = \left(\frac{3}{2}\Delta x \;\; \frac{3}{2}\Delta y \;\; \Delta z \right)^{\frac{1}{3}}. \tag{3}$$

However, for the stable stratification considered here, $\ell = \min(\Delta, \ell_{st})$, where ℓ_{st} is Deardorff's (1980) length scale that accounts for reduced mixing imposed by stratification $\ell_{st} = 0.76 \left(\frac{e}{\beta \partial_z \theta}\right)^{\frac{1}{2}}$. The isotropy factor $\gamma = S'/(\langle S \rangle + S')$ where $(\langle S \rangle, S')$ are the resolved strain rate average and fluctuation, respectively; the strain rate average is over an x–y plane. The isotropy factor essentially reduces the length scale ℓ as the wall is approached depending on the magnitude of the resolved turbulence fluctuations. The boundary conditions, solution algorithm, and further details are provided in Sullivan et al. (2016).

Simulation configuration and methods:

GABLS1 is a canonical high-latitude SBL driven by constant geostrophic winds $U_g = 8$ m s^{-1} with Coriolis parameter $f = 1.39 \times 10^{-4}$ s^{-1} above a horizontally homogeneous rough surface with roughness length $z_o = 0.1$ m. LES are performed using a mixed pseudo-spectral discretization in horizontal planes and second-order centered finite difference in the vertical direction (Sullivan et al., 1994). The simulations are initiated from a neutral state with an overlying stable inversion $\partial_z \theta = 0.01$ K m^{-1} imposed at an initial height $z = 100$ m. The computational domain size is $(400 \times 400 \times 400)$ m. A constant rate of surface cooling $C_r = 0.25$ K h^{-1} is applied starting at $t = 0$ s to generate stably stratified turbulence. The specification of surface temperature fully couples the momentum and temperature relations in the Monin–Obukhov bottom boundary conditions, which is a more demanding test for LES compared to a specified temperature flux: further description of the simulation design is given in Sullivan et al. (2016). Previous GABLS1 simulations

Table 1: Bulk simulation properties, with entries: LES case, mesh points N, cooling rate C_r, mesh spacing $\triangle = \Delta x = \Delta y = \Delta z$, friction velocity u_*, temperature flux Q_*, boundary layer height h, Monin-Obukhov stability length $L_{mo} = -u_*^3/\kappa\beta Q_*$, boundary layer stability h/L_{mo}.

Case	N	C_r (K hr^{-1})	$\triangle$ (m)	u_* (m s^{-1})	$Q_* \times 10^3$ (K m s^{-1})	h (m)	L_{mo} (m)	h/L_{mo}
C2	2048^3	0.25	0.20	0.249	-8.83	187.2	118.6	1.56

find a quasi-steady SBL featuring a low-level jet with wind profile veering in the SBL after 8 hours of simulation; the SBL depth $h \approx 200$ m, the surface temperature flux $Q_* \approx -9$ K m s^{-1}, and friction velocity $u_* \approx 0.25$ m s^{-1}, which vary with the mesh resolution (Sullivan et al., 2016). The GABLS1 SBL is weakly stable with continuous turbulence and the boundary-layer stability metric is $h/L_{mo} \sim 1.7$, where $L_{mo} \approx 118$ m is the Monin–Obukhov length; see Table 1.

The present work expands on Sullivan et al. (2016) using an unprecedented resolution of $\triangle \approx 0.2$ m in all three directions with a mesh of $N = 2048^3$. Because of the computational cost a two-step recipe is used to perform the LES. First, a seed simulation with $N = (512 \times 512 \times 2048)$ is run from scratch for 8 hrs. The grid in this seed simulation is anisotropic but has the advantage that the wind and temperature profiles vary smoothly in the vertical direction. Next, the last volume from the seed simulation is archived and the field variables are interpolated in the horizontal x-y directions using zero padded Fourier transforms to generate a restart volume with $N = 2048^3$ points. The fine mesh solution is then started and run for an additional 0.5 hr. Having reached approximate quasi-steady state, the simulation is run for another 0.5 hr at constant time-step of $\Delta t = 0.015$ s for ingestion into JHTDB.

Data available

The available data include the three LES-resolved velocity components $\overline{u}(x,y,z,t)$, $\overline{v}(x,y,z,t)$, $\overline{w}(x,y,z,t)$, pressure $\overline{p}(x,y,z,t)$, potential temperature $\overline{\theta}(x,y,z,t)$, and subgrid-scale kinetic energy $e(x,y,z,t)$. The variable locations are vertically staggered, with $\overline{u}$, $\overline{v}$, $\overline{\theta}$, and $\overline{p}$, located at the half-level (i.e. starting from $\Delta z/2$), and $\overline{w}$ and $\overline{e}$ located at the full-level (i.e. starting from Δz).

Two classes of data are available: time-resolved during a relatively short period of time consisting of 100 time-steps separated by 0.075 seconds (high-frequency dataset name: "SABL2048high"), and 20 statistically independent snapshots separated by ~ 90 seconds (low-frequency dataset name: "SABL2048low").

The stored data are provided in SI units (i.e. x,y,z positions in meters, velocities in m s^{-1}, temperature in Kelvin, and SFS energy in m^2 s^{-2}). In the database, potential temperature is stored relative to the reference temperature $\theta_{\text{ref}} = 265$ K.

Flow statistics

In order to document the first- and second-order statistics, they are measured from the entire "SABL2048low" dataset, i.e. averaging over 20 independent snapshots, and over the spanwise and streamwise directions. Resulting vertical profiles of mean velocity and temperature are provided in Fig. 1. Profiles of second-order

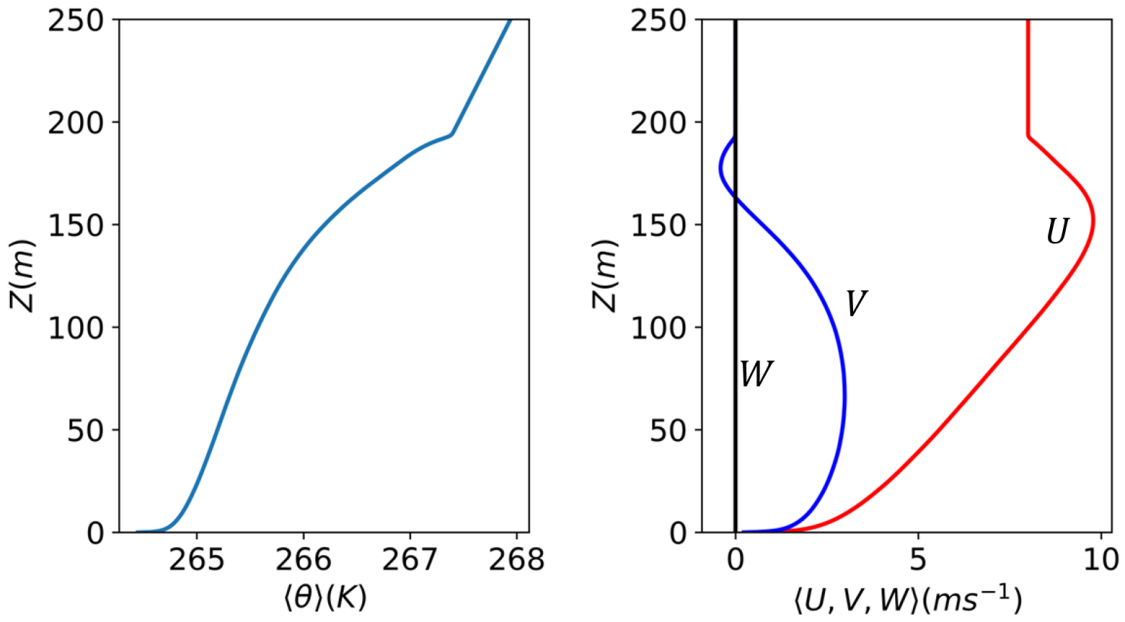

Figure 1: Vertical profiles of average temperature θ (left panel). Vertical profiles of average winds U,V,W (right panel).

statistics are shown in Figs. 2 and 3 (left panel). These figures can be compared to those appearing in McWilliams et al. (2023) that were computed from twice as long data and are therefore slightly better converged and smoother. Fluctuations are defined and computed as deviations from instantaneous horizontal means, e.g. $u' = u - \langle u \rangle_{xy}$, in order to exclude slow temporal variability (e.g. due to inertial oscillations) from the turbulence statistics. Also, turbulent heat flux and shear stresses are presented here without adding the SFS fluxes.

Fig. 3 (right panel) shows the profile of mean SGS kinetic energy relative to the total turbulent kinetic energy. Profiles of average Richardson number ($Ri(z) = N^2/S^2$) and average shear ($S^2 = (\partial \langle u_\perp \rangle / \partial z)^2$, where $\langle \mathbf{u}_\perp \rangle = U\hat{\mathbf{i}} + V\hat{\mathbf{j}}$) and buoyancy frequency squared [$N^2 = (g/\theta_{\text{ref}})\,\partial_z \langle \theta \rangle$] are provided in Fig. 4.

Acknowledgements: We acknowledge funding by the National Science Foundation (NSF award number 2103874 with the JHU to NSF NCAR, subaward 2005117865). Computational resources were provided by NSF NCAR's Computational and Information Systems Laboratory (2019, 2023).

(1) *Note:* The divergence-free condition in the simulation is enforced based on the spectral representation of the derivatives on horizontal planes. The JHTDB analysis tools for gradients are based on finite differencing of various orders. Therefore, when evaluating the divergence using these spatially more localized derivative operators, a non-zero divergence should be expected.

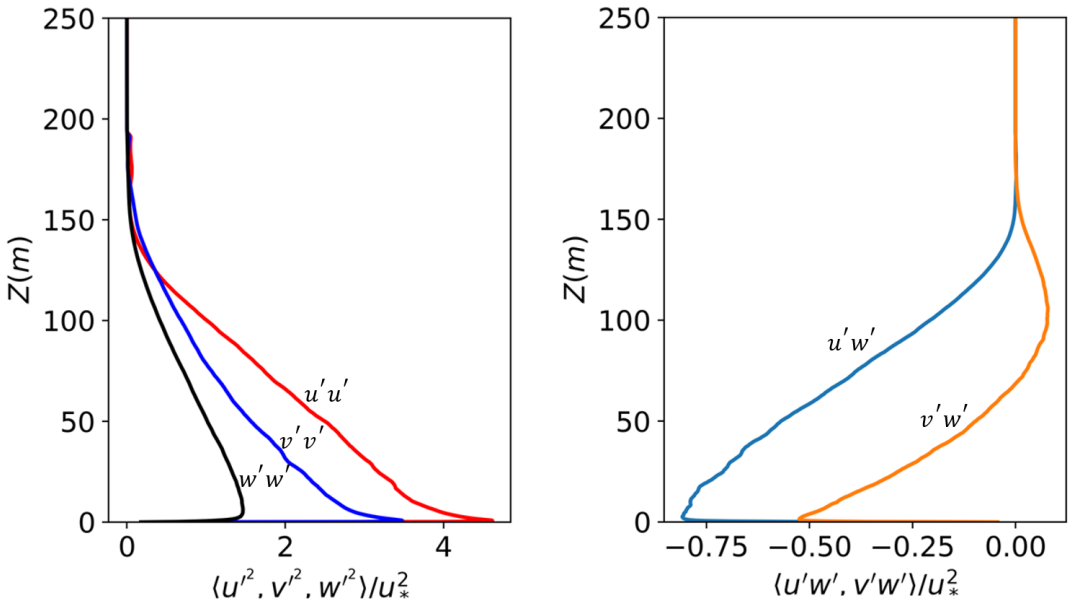

Figure 2: Vertical profiles of velocity variances $\langle u'^2, v'^2, w'^2 \rangle / u_*^2$ (left panel). Vertical profiles of cross velocity variances $\langle u'w', v'w' \rangle / u_*^2$ (right panel).

References

Beare, R. J., and Coauthors, 2006: An intercomparison of large-eddy simulations of the stable boundary layer. *Bound.-Layer Meteorol.*, **118**, 242–272, doi:10.1007/s10546-004-2820-6.

Computational and Information Systems Laboratory: Cheyenne: HPE/SGI ICE XA System (NCAR Community Computing). Boulder, CO: NSF National Center for Atmospheric Research, doi:10.5065/D6RX99HX.

Computational and Information Systems Laboratory: Derecho: HPE Cray EX System (NCAR Community Computing). Boulder, CO: NSF National Center for Atmospheric Research, doi:10.5065/qx9a-pg09.

Deardorff, J. W., 1980: Stratocumulus-capped mixed layers derived from a three-dimensional model. *Bound.-Layer Meteorol.*, **18**, 495–527.

Holtslag, A. A. M., 2006: GEWEX atmospheric boundary-layer study GABLS on stable boundary layers. *Bound.-Layer Meteorol.*, **118**, 243–246, doi:10.1007/s10546-005-9008-6.

Huang, J., and E. Bou-Zeid, 2013: Turbulence and vertical fluxes in the stable atmospheric boundary layer. Part I: A large-eddy simulation study. *J. Atmos. Sci.*, **70**, 1513–1527, doi:10.1175/JAS-D-12-0167.1.

McWilliams, J. C., C. Meneveau, E. G. Patton, and P. P. Sullivan, 2023: Stable boundary layers and subfilter-scale motions. *Atmosphere*, **14 (7)**, 1107, doi:10.3390/atmos14071107.

Moeng, C.-H., and P. P. Sullivan, 2015: Large-eddy simulation. *Encyclopedia of Atmospheric Sciences 2nd*

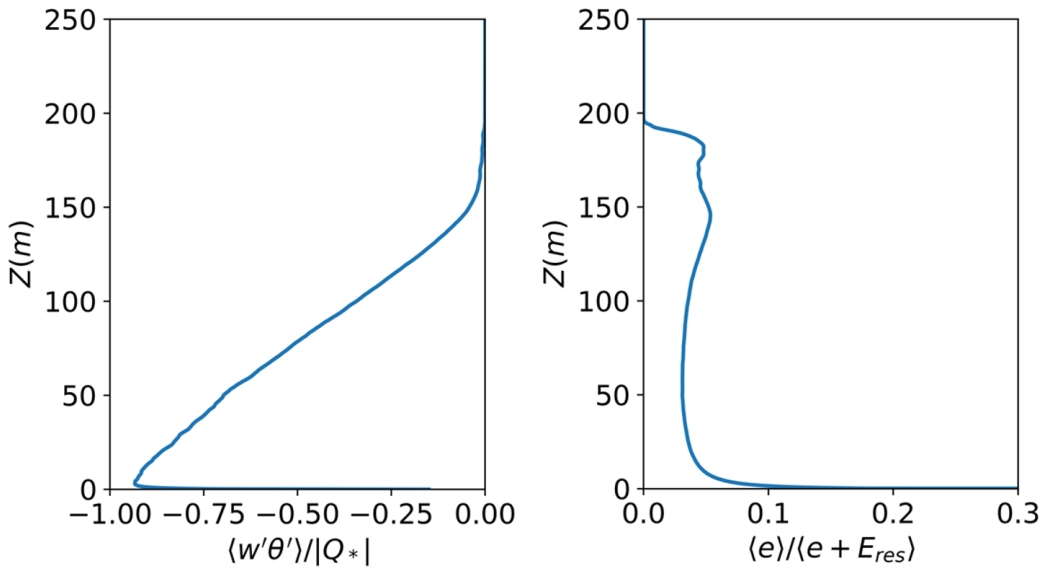

Figure 3: Vertical profiles of average temperature flux $\langle w'\theta' \rangle / |Q_*|$ (left panel). Vertical profiles of SFS energy in the LES as a fraction of the total energy $\langle e \rangle / \langle e + E_{res} \rangle$ (right panel).

Edition, G. R. North, F. Zhang, and J. Pyle, Eds., Vol. 4, Academic Press, 232–240, doi:10.1016/B978-0-12-382225-3.00201-2.

Sullivan, P. P., J. C. McWilliams, and C.-H. Moeng, 1994: A subgrid-scale model for large-eddy simulation of planetary boundary-layer flows. *Bound.-Layer Meteorol.*, **71**, 247–276, doi:10.1007/BF00713741.

Sullivan, P. P., J. C. Weil, E. G. Patton, H. J. J. Jonker, and D. V. Mironov, 2016: Turbulent winds and temperature fronts in large-eddy simulations of the stable atmospheric boundary layer. *J. Atmos. Sci.*, **73**, 1815–1840, doi:10.1175/JAS-D-15-0339.1.

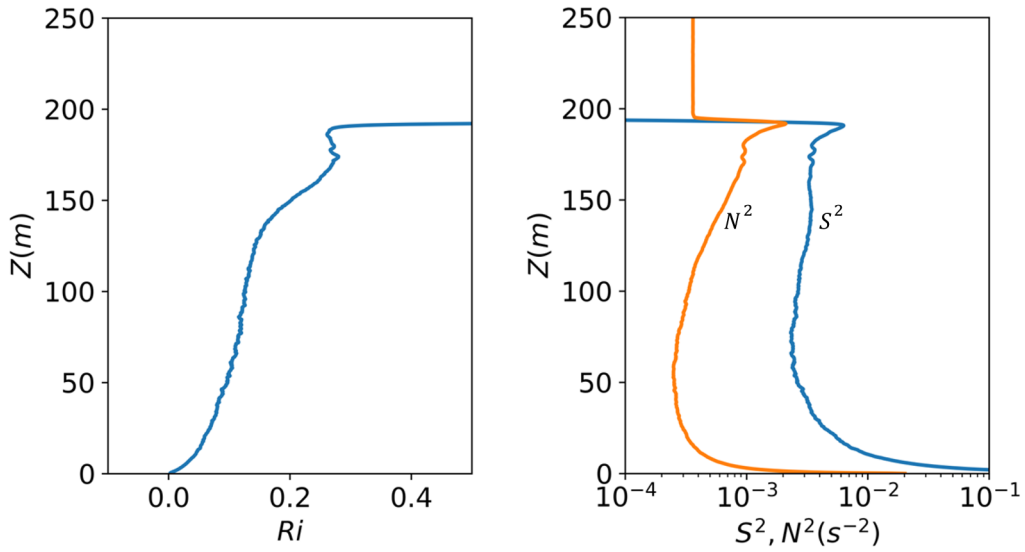

Figure 4: Vertical profiles of average Richardson number (left panel). Vertical profiles of average shear and buoyancy frequency squared S^2, N^2 (right panel).